Return Map for the Chaotic Dripping Faucet

P. COULLET,[1,*] L. MAHADEVAN[2,**] and C. RIERA[1,***]

[1] *Institut Non Lineaire de Nice, UMR CNRS 129*
1361, Route des Lucioles, 06560 Valbonne, France
[2] *Department of Mechanical Engineering, 1-310*
M.I.T., 77 Mass. Ave., Cambridge, MA 02139, USA

We propose a simple model for the chaotic dripping of a faucet in terms of a return map constructed by analyzing the stability of a pendant drop. The return map couples an Andronov saddle-node bifurcation corresponding to the instability of the drop whose volume exceed a critical value, and a Shilnikov homoclinic bifurcation induced by the presence of a weakly damped oscillatory mode. We show that the predictions of the return map are qualitatively consistent with the experimental results. We compare these results with those of a delay map constructed from the solution of an asymptotic lubrication model for the evolution of the dripping faucet.

§1. Introduction

Drop formation is an everyday phenomena. The first scientific study of drops is possibly due to Mariotte [1] who noticed that a steam of water flowing from a faucet breaks into drops. Like many authors after him, he thought that gravity and external forces are responsible for this process. It was only much later that Laplace [2] and Young [3] discovered that surface tension is the source of the instability. The subject has remained active since the middle of the last century, starting with the studies of Plateau and Rayleigh through recent times where there have been a large number of works on related problems in the context of the analysis of singularities in free-surface flows. [4] Here we focus on an aspect of this problem that provided a stimulus to early studies on chaos, [5] the transition to chaotic dripping in a faucet. This last problem has been the subject of many experimental and theoretical papers (see Innocenzo [6] for a recent example along with a review of earlier work). However most of these papers have modeled the system as a relaxation oscillator using phenomenologically motivated models. Our aim is to provide a minimal model based on fluid mechanics to describe the dynamics of a dripping faucet.

§2. Stability and bifurcation of a pending drop

In order to do so, we first consider the case when the flow rate is very small, the drop is considered to be static and remains attached to the faucet until its volume exceeds a threshold V_c. For a narrow faucet of radius R, drops with a volume less than V_c are stable and axisymmetric; [7),8] for wider faucets, one can have non

*) Professeur à l'institut universitaire de France. E-mail address: coullet@inln.cnrs.fr
**) E-mail address: l_m@mit.edu
***) E-mail address: riera@inln.cnrs.fr

axisymmetric stable drops,[9] leading to more complex dripping patterns. The shape of an axisymmetric pendant drop is determined by the minimizing its energy which consist of a gravitational part and a surface tension part subject to the constraint of a constant volume. It is described by the well-known Laplace-Young equation.[8] Equivalently, one may write down an equation for the balance of the vertical forces, along with some kinematic equations for the shape of the interface, leading to a set of a first order ordinary differential equations (ODE) which read[10]

$$\begin{cases} \dfrac{d\theta}{ds} = \dfrac{\cos\theta}{r} - \dfrac{z}{l_0^2}, \\ \dfrac{dz}{ds} = -\cos\theta, \\ \dfrac{dr}{ds} = \sin\theta. \end{cases} \tag{2·1}$$

Here the variables r, s, θ and z are defined in Fig. 1, and the capillary length is $l_0 = \sqrt{\Gamma/\rho}$ for a fluid drop with surface tension Γ, and a density ρ in a gravitational field g. The boundary condition at the top of the drop near the faucet are unknown, but at the bottom of the drop they are $r(0) = 0$, $\theta(0) = \pi/2$ and $z(0) = P_b/\rho g$, i.e., P_b is the unknown hydrostatic pressure at the bottom of the drop; it is our control parameter for the set of ODE. Choosing a value for P_b, we integrate (2·1) as an initial value problem until we satisfy the boundary condition $r = R$, where R is the radius of the faucet in term of capillary length. We use a shooting method to determine P_b for a given volume $V = \int \pi r^2 dz$. We may obtain several values of P_b for a given volume, only the first with $dz(0)/dV > 0$, which correspond to the branch starting at the origin, is stable[8] (see Fig. 2), so there is a critical volume V_c above which the drop is unstable as its weight is larger the force due to surface tension. This instability corresponds to the "collision" of a static stable and unstable solution for $V = V_c$. This is, in fact, the signature of a saddle-node bifurcation.

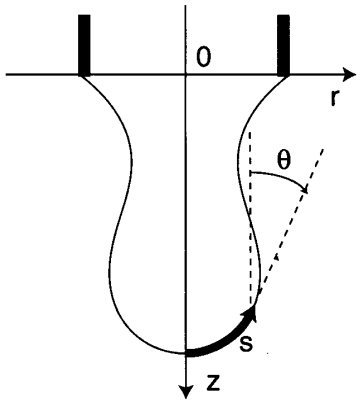

Fig. 1. Definition of the variables for the set of ODE's.

To understand the mechanism of this linear instability dynamically, we have to consider the hydrodynamical equations linearized about a stationary solution. Instead of using the complete Navier-Stokes equations in the case of Eulerian one-dimensional lubrication theories,[11] we simplify the analysis by using a new lubrication model embodied in a Lagrangian approach for the fluid.[10] The main assumptions are the following: the drop remains axisymmetric during its motion, the radial component of the fluid velocity is negligible compared to the axial component which depends only on z, and there is no overturning of the interface which is assumed

to be a graph in the axial variable z. These assumptions correspond to lubrication theory and are asymptotically valid for slender drops of large viscosity. Recent simulations of the resulting low-order equations [10] have shown good agreements with experiments even for fairly squat drops of low viscosity. The above assumptions lead to the conclusion that there is no exchange of fluid between neighboring horizontal slices of the drop, so that the volume of a slice is constant during motion and can be treated as a Lagrangian variable. This leads to a Lagrangian hydrodynamical description that is essentially equivalent to earlier Eulerian description. Explicitly, the volume between the bottom of the drop $z_b(t)$ and z is

$$\xi(z,t) = \int_z^{z_b(t)} \pi r(\zeta,t)^2 d\zeta, \quad (2\cdot2)$$

where r is the radius of the drop. In terms of the Lagrangian variable $\xi(z,t)$, we can write the kinetic, potential and surface tension energy of the system as

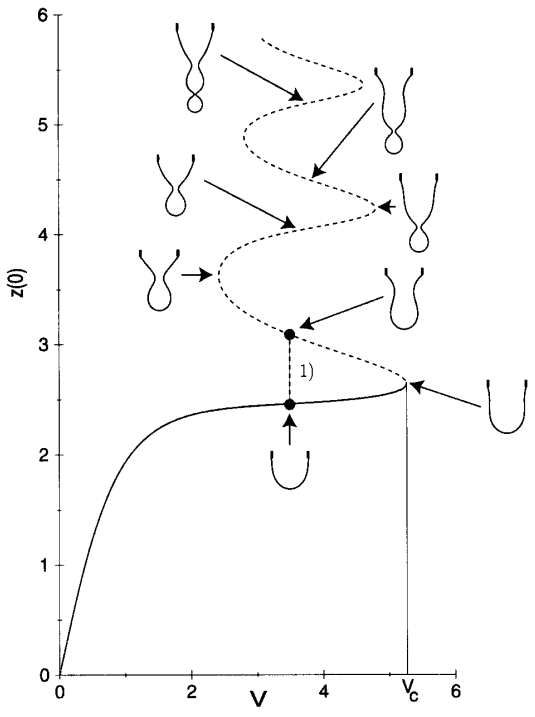

Fig. 2. The initial condition $z(0)$ versus the volume of the drop. The dashed line corresponds to unstable stationary drops, the solid line to the stable drops. V_c is the maximum volume of a stable stationary drop, above this volume, there is no stable stationary pendant drop. The saddle-node bifurcation occurs for $V = V_c$. 1) is an example with two drops that have the same volume not the same shape and consequently the same pressure at their bottom P_b.

$$\begin{cases} E_{\rm kin} &= \frac{\rho}{2}\int_0^{\xi_0(t)} \left(\frac{\partial z(\xi,t)}{\partial t}\right)^2 d\xi, \\ U_g &= -\rho g \int_0^{\xi_0(t)} z(\xi,t) d\xi, \\ U_\Gamma &= \Gamma \int_0^{\xi_0(t)} \sqrt{4\pi z' + \frac{(z'')^2}{(z')^4}}\, d\xi. \end{cases} \quad (2\cdot3)$$

Here $E_{\rm kin}$ is the kinetic energy, U_g the potential energy, U_Γ the surface tension energy, $\xi_0(t)$ is the total volume of the drop at the time t, and a prime corresponds to partial derivative against the Lagrangian variable ξ. Then we can write the Lagrangian of the system as

$$\mathcal{L} = E_{\rm kin} - U_g - U_\Gamma. \quad (2\cdot4)$$

The effect of viscosity is then expressed by a Rayleigh dissipation function,

$$\dot{E}_{\rm kin} = -3\eta \int_0^{\xi_0(t)} \left(\frac{v'(\xi,t)}{z'(\xi,t)}\right)^2 d\xi. \quad (2\cdot5)$$

Here v is the velocity and η is the dimensionless viscosity in units of $\eta_0 = (\rho\Gamma^3/g)^{1/4}$ (for water at 20°C, $\eta_0 = 1.627\text{g}\cdot\text{cm}^{-1}\text{s}^{-1}$ and $\eta = 0.002$), and this expression corresponds to the dissipation rate in purely extensional flow. Then, Lagrange's equation for the system is

$$\frac{d}{dt}\frac{\partial \mathcal{L}}{\partial v} = \frac{\partial \mathcal{L}}{\partial z} + \frac{1}{2}\frac{\partial \dot{E}_{\text{kin}}}{\partial v}. \tag{2·6}$$

For the purposes of computation, we discretize the Lagrangian spatially in term of variables that characterize each slice of fluid, the position z_i, the velocity $v_i = \frac{\partial z_i}{\partial t}$ and the mass m_i, so that for a drop sliced into N disks, we get an N dimensional dynamical system. The discretized version of each term in the Lagrangian reads

$$\begin{cases} E_{\text{kin}} \simeq \frac{1}{2}\sum_{i=1}^{N} m_i v_i^2, \\ U_g \simeq -g\sum_{i=1}^{N} m_i z_i, \\ U_\Gamma \simeq \Gamma\sum_{i=1}^{N} \frac{\pi}{2}(r_i + r_{i+1})\sqrt{(z_{i+1}-z_{i-1})^2 + (r_i - r_{i+1})^2}, \\ \dot{E}_{\text{kin}} \simeq -3\eta\sum_{i=1}^{N}\left(\frac{v_i - v_{i-1}}{z_i - z_{i-1}}\right)^2 m_i, \end{cases} \tag{2·7}$$

where $r_i = \sqrt{\frac{m_i}{\pi(z_i - z_{i-1})}}$ is the average radius of the disk number i. This leads to the N equations of motion for each of the disks.

$$\frac{d}{dt}\frac{\partial \mathcal{L}}{\partial v_i} = \frac{\partial \mathcal{L}}{\partial z_i} + \frac{1}{2}\frac{\partial \dot{E}_{\text{kin}}}{\partial v_i}, \quad i = 1, N. \tag{2·8}$$

We can linearize (2·8) numerically in the neighborhood of stationary solutions of (2·1) and studying the spectrum $\omega_i, i = 1, N$ of the resulting system. We find that when $V < V_c$ and for stationary drops of the branch starting at the origin Fig. 2, all eigenvalues are complex conjugate with negative real part. So these drops are stable and possess several damped oscillations modes. These modes correspond to standing wave that may exist along the surface of the drop

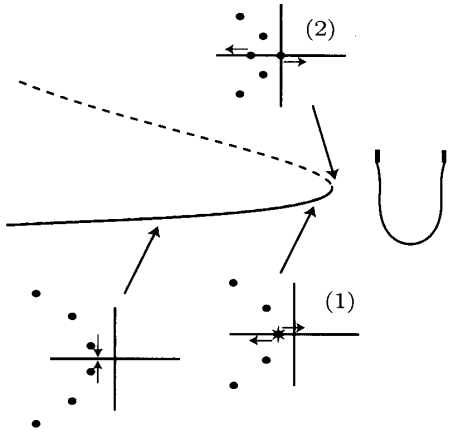

Fig. 3. Enlargement of spectrum near the origin for some representative points close to V_c; the critical damping for the first oscillation mode the drop is shown in (1), and the onset of the saddle-node bifurcation is shown in (2), and the leading eigenvalues for (2) are $\lambda_1 = 0$ and $\lambda_2 = -0.017 \pm i3.468$ for water.

due to some disturbances. When $V \approx V_c$ two complex conjugate eigenvalues become real and after one of them crosses the imaginary axis when $V = V_c$. The collision of the first couple of complex eigenvalues with the real axis corresponds to critical damping of the first oscillation mode, i.e. the global oscillation of the drop. When $V > V_c$, the stationary drop loses its stability by a saddle-node bifurcation, as can be seen in Fig. 3.

§3. Dynamic of the dripping faucet with flow rate

Now we consider the faucet with a flow rate, and we consider the dripping faucet characteristic quantities. The fluid velocity inside the faucet of radius R is noted v_0, and we use it in the following to characterize flow rate. The time scale for the formation of a pendant drop is $\tau_f \sim \frac{R}{v_0}$. Once the volume of the pendant drop reaches V_c, the drop becomes unstable via a saddle-node bifurcation as we saw first, and forms a neck which quickly narrows down until a droplet pinches off in finite time. This process occurs in a time $\tau_n \sim \sqrt{\rho R^3/\Gamma}$,[4] independent of the flow rate, and much more rapidly than the time for a drop to form. After a droplet pinches off, the remaining liquid retracts under the influence of surface tension, and depending on the fluid and the flow rate, one can have the formation of very small droplets called satellite during this process. At the end of this process, the remaining drop oscillate with a characteristic frequency $f = \sqrt{8\Gamma/3\pi\rho\mathcal{V}}$,[12] where $\mathcal{V}$ is the volume of the last remaining droplet. Since the volume of the pendant drop grows steadily due to the constant flow rate, the frequency decreases and the oscillations are damped out by viscous fluid motion at a rate $1/\tau_d \sim \sqrt{2\pi f\eta}/\mathcal{V}^{1/3}$. The global oscillation frequency and its decay rate are find again in the linear analysis of stationary pendant drop, and are correspond to the eigenvalues complex conjugate close to the origin. For very small flow rates, these oscillations can be considered as completely damped out by the time the pendant drop attains the critical volume V_c. In this case, droplets are emitted from the faucet with a constant period, the time for the drop to become unstable is constant. As the flow rate is increased, these partially damped oscillations modify the onset of the instability characterized by a saddle-node bifurcation, the drop can overcome the nucleation variety, which characterizes the presence of the saddle-node bifurcation, before or after the drop reaches its critical volume. Equivalently, the dimensionless ration of the filling time to the damping time τ_n/τ_d advances or delays the onset of the necking and is responsible for the variation of the periodicity (or lack thereof) of drop emission. The stability properties of the drop near its critical volume seems to be the unique responsible for the special dynamic of chaotic dripping faucet. For instance, as the flow rate is gradually increased from nul flow rate, the constant periodicity "drop-drop" gives way to a "drop-drip" scenario via a period-doubling bifurcation as follows. Once the first pendant drop reaches the critical volume V_c, a large droplet "drops" leading to a highly elongated residual filament and small remaining volume. If the flow rate is large enough so that the oscillations are not completely damped out, the next droplet may become unstable when $V < V_c$, so that it "drips", leading to smaller residual filament and larger remaining volume whose oscillations will be damped out

much sooner, thereby (possibly) allowing the pendant drop reach its maximum size V_c before it "drops", and so.

In order to built a low-dimensional dynamical system mimicking (2·8), we can solve it numerically over a time much longer than the time for the pinch off of a single droplet, for instance three or four in the case of periodic dripping, to have a clear phase space, to achieve this, we need an order parameter that is continuous through the pinch off process. We cannot use the volume or the length of the drop which do not satisfy this criterion. However, the radius of the drop at an appropriate location, i.e., above the region where drops are usually cut, suffices and allows us to rebuilt phase space by the delay method.[13] This allows us to see the different time scale of the dripping dynamic and the role of the saddle-node region and the damped oscillations near this region.

We show such a reconstruction in Fig. 4, and observed that there are two qualitatively different regions: a large excursion corresponding to the dynamic that leads to the droplet pinch-off, and a much more compact region corresponding to the damped oscillations following a pinch-off event, that eventually leads the orbit to the neighborhood of the saddle-node area whence it escapes again.

The large excursion in the phase-space is quick compared to the time to form drop. The time of this excursion does not depend on the flow rate and is done in a self-similar manners. It does not influence the time for a drop to fall, and consequently this excursion is unimportant compared to the flow near the saddle-node area. In this region the dynamic time scale is given by the interval between the critical value and the bifurcation parameter, in our case $\sqrt{\epsilon}$. At last the role of damped oscillations is to modify the approach of the saddle-node region and consequently the time for

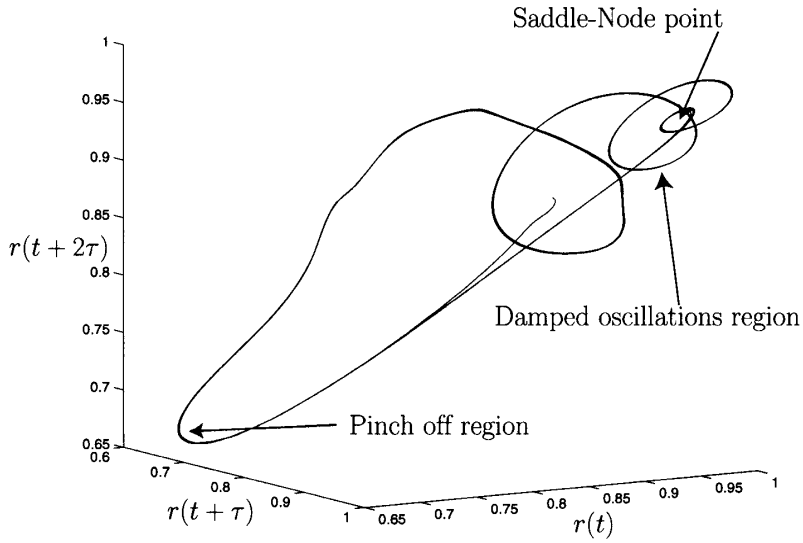

Fig. 4. Reconstruction of the flow by the time delay method, obtained by solving (2·8) numerically. The radius of the drop is taken at the position $z = 0.5$, it is always continue during the process. The parameter used for the simulation corresponds to a fluid 10 times more viscous than water flowing out of a faucet of diameter $R = 1$ at a flow rate $v_0 = 0.01$ (in dimensional terms, $R = 2.6$ mm and the flow rate is $0.015\text{cm}^3 \cdot \text{s}^{-1}$). We observe a long excursion followed by a damped oscillations before the orbit returns to the neighborhood of the saddle-node point.

drop to fall.

§4. Construction of the return map

Since the dynamical properties of the dripping faucet are controlled by the behavior of the system close to the saddle-node bifurcation, and not by the pinch-off process, we can construct a simple model which describes an oscillatory damped mode and a saddle-node bifurcation in the spirit of the Andronov original paper, [14] which are the main points of this chaotic dynamic.

$$\begin{cases} \partial_t U &= (i\omega - \lambda)U, \\ \partial_t Z &= \epsilon + Z^2, \end{cases} \tag{4·1}$$

where $U = X + iY$ is the amplitude of the oscillatory damped mode with eigenvalue $i\omega - \lambda$, with $\omega, \lambda > 0$, and $\epsilon > 0$ is the saddle-node bifurcation parameter. In the context of hydrodynamical theory, U and Z are similar to a Galerkin approximation of the complete dynamic, ω is the scaled pendant drop oscillations frequency and λ the scaled rate of decay of these oscillations (in units of $1/t_0$, with $t_0 = (\Gamma/\rho g^3)^{1/4}$), while ϵ is the scaled flow rate (in units of l_0^3/t_0). ω and λ are computed in using the previous linear analysis. In order to complete the construction of the dynamical model, we need a global reinjection process that mimics the complex dynamics of a self-similar pinch-off of a droplet. [4),15] In light of Fig. 4, the details of this process are unimportant to understand the chaotic behavior of dripping faucet, the role of this process is just to bring back the flow near the saddle-node region in the phase space. We now proceed to give an explicit construction of this dynamical system [16] in terms of a return map around a parallelopiped of length (A, A, B), centered at the saddle-node point, as shown in Fig. 5, i.e., we focus one's attention on the area of the phase space which is responsible of the diversity of this dynamic.

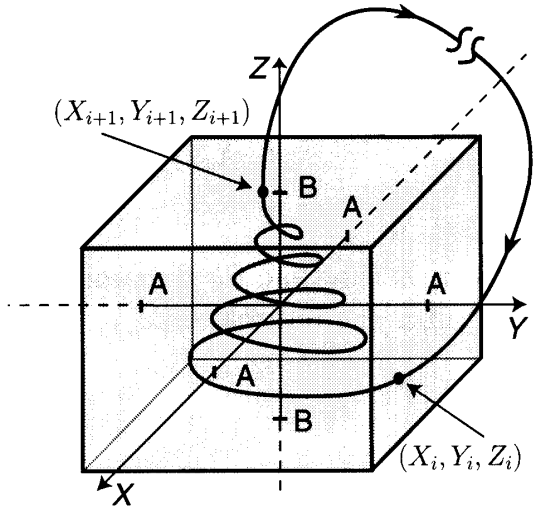

Fig. 5. A parallepopiped around the saddle-node in phase-space is used to construct the mapping from the plane before the bifurcation to the plane after the bifurcation. A simple rigid transport is used to model the global reinjection process associated with the complex dynamics of pinch-off, recoil and growth. The details of this process are unimportant for the study of dripping faucet chaotic behavior.

We first construct the mapping from the plane $Y = A$, before saddle-node aera, to the plane $Z = B$, after saddle-node area. A point (X_i, A, Z_i) is mapped into (X_{i+1}, Y_{i+1}, B),

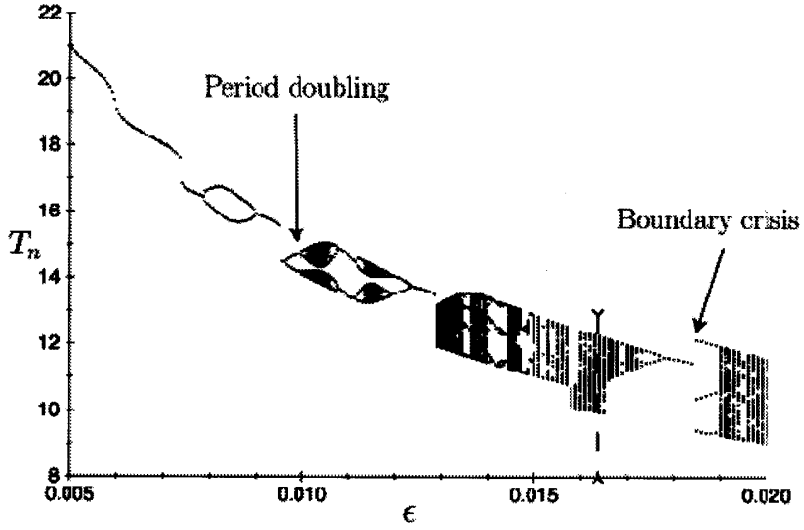

Fig. 6. For small flow rate, the dripping is periodic. For intermediate flow rate, the dripping may be chaotic. The transition to chaos can be by period doubling bifurcation (for instance $\epsilon = 0.01$), or the result of boundary crisis (for instance $\epsilon = 0.0125$).

$$\begin{cases} X_{i+1} &= (X_i \cos(\omega\tau_i) - A\sin(\omega\tau_i))e^{-\lambda\tau_i}, \\ Y_{i+1} &= (X_i \cos(\omega\tau_i) + A\sin(\omega\tau_i))e^{-\lambda\tau_i}, \end{cases} \tag{4·2}$$

where τ_i is the time for dynamic to go from the plane before the bifurcation to the plane after the bifurcation,

$$\tau_i = \frac{\arctan(B/\sqrt{\epsilon}) - \arctan(Z_i/\sqrt{\epsilon})}{\sqrt{\epsilon}}. \tag{4·3}$$

The simplest way to model the reinjection flow is via a rigid transport, as for instance

$$\begin{cases} X_{i+1} \to X_{i+1}, \\ Y_{i+1} \to Z_{i+1}. \end{cases} \tag{4·4}$$

Using (4·2) and (4·4), the Poincaré map which models the process is then given by

$$\begin{cases} \tau_i &= \dfrac{\arctan(B/\sqrt{\epsilon}) - \arctan(Z_i/\sqrt{\epsilon})}{\sqrt{\epsilon}}, \\ X_{i+1} &= (X_i \cos(\omega\tau_i) - A\sin(\omega\tau_i))e^{-\lambda\tau_i}, \\ Z_{i+1} &= (X_i \cos(\omega\tau_i) + A\sin(\omega\tau_i))e^{-\lambda\tau_i}. \end{cases} \tag{4·5}$$

Now we can use numerical simulations of (4·5) and compare with results of other simulations and experiments (for instance see Ref. 18), etc.). This reveals that for small flow rate all the orbits converge towards a fixed point which describes a periodic dripping process. The same phenomenon appears for a large flow rate it represents

a transition from dripping to jetting.[20] For intermediate flow rate, chaotic behavior is observed with different type of transition. These aspects are all shown in Fig. 6.

The structure of the map is self explanatory. As ϵ increases, the observed chaos is connected with the formation a classical Smale horseshoe. Depending on the value of other parameters such as Z_i and X_i, for a larger ϵ the attractor takes the appearance of a spiral, corresponding to a horseshoe with more symbols. The transition to chaos occurs either by successive period doubling bifurcations or by the collision between a chaotic attractor and an unstable fixed point via a *boundary crisis* and is responsible for the sudden changes in the attractor,[21] similar to that observed in experiments.

§5. Conclusion

We conclude by a brief discussion of our results. On the basis of the study of the stability of pendant drop and numerical simulations of a lubrication-type model for the hydrodynamic of a dripping faucet, we constructed the simplest rational return map characterizing the Andronov-Shilnikov bifurcation that accounts for the various experimentally observed behaviors of a dripping faucet, such as the different transitions to chaos, the shape of the attractor as shown in Fig. 7, etc. In contrast with other dripping faucet return map based on experimental results, our model assumes that the complex dynamics of the dripping faucet is induced by the coupling between a saddle-node bifurcation (responsible of drop falling) and a damped oscillation mode which corresponds to the reaction of the drop after a pinch-off event. The dripping faucet dynamical properties do not depend on the pinch-off event on the stability properties near the critical volume. Improvements in the model are currently underway and can take two paths. First a Galerkin projection of the drop dynamics will give us a better estimate than the linear analysis of the frequency and damping rate of the oscillatory damped motion. Second, the reinjection process can be modelled more realistically in using, for example, a contraction parameter with

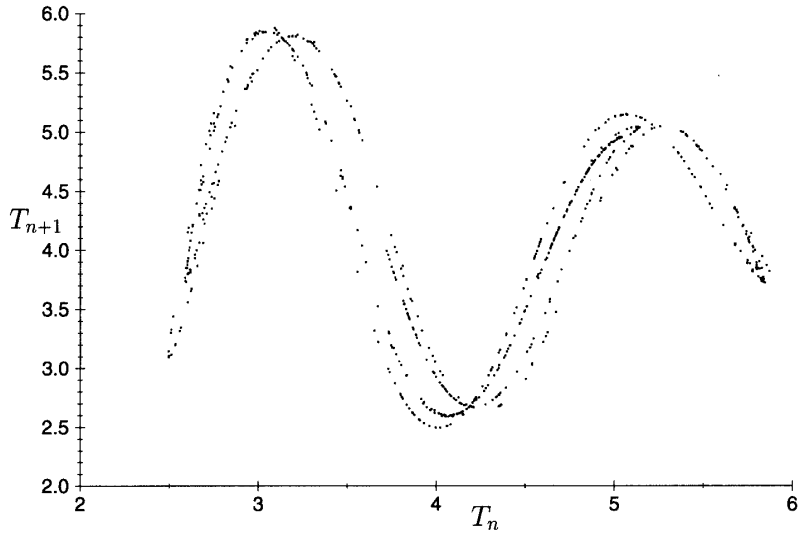

Fig. 7. Return map: plot of the time interval between two consecutive drops T_{n+1} and the last time interval T_n. This is a characteristic of the chaos in the dripping faucet experiment.

the rigid transport. This model sets up the framework for a study of the problem of chaotic nucleation in other dynamical systems.

References

1) E. Mariotte, *Traité du mouvement des eaux et des autres corps fluides* (E. Michallet, Paris, 1686).
2) P. S. Laplace, *Méchanique céleste, suppl. au livre X* (1805).
3) T. Young, Philos. Trans. R. Soc. London **95** (1805), 65.
4) J. Eggers, Rev. Mod. Phys. **69** (1997), 865.
5) R. S. Shaw, *The dripping faucet as a model chaotic system* (Aerial Press, 1984).
6) A. D'Innocenzo and L. Renna, Phys. Rev. **E55** (1997), 6676.
7) J. F. Padday and A. R. Pitt, Philos. Trans. R. Soc. London **A275** (1973), 489.
8) E. Pitts, J. Inst. Math. Appl. **17** (1976), 387.
9) D. H. Michael and P. G. Williams, Proc. R. Soc. London **A351** (1976), 117.
10) N. Fuchikami, S. Ishioka and K. Kiyono, J. Phys. Soc. Jpn. **68** (1999), 1185.
11) J. Eggers and T. F. Dupont, J. Fluid Mech. **262** (1994), 205.
12) M. S. Longuet-Higgins, B. R. Kerman and K. Lunde, J. Fluid Mech. **230** (1991), 365.
13) J. P. Eckmann and D. Ruelle, Rev. Mod. Phys. **57** (1985), 617 .
14) A. Andronov and M. Leontovich, J. State Univ. Gorki **6** (1937), 3.
15) J. Eggers, Phys. Rev. Lett. **71** (1993), 3458.
16) A. Arneodo, P. Coullet, E. A. Spiegel and C. Tresser, Physica **D14** (1985), 327.
17) L. Renna, Phys. Lett. **A261** (1999), 3.
18) T. Katsuyama and K. Nagata, J. Phys. Soc. Jpn. **68** (1999), 1185.
19) K. Dreyer and F. R. Hickey, Am. J. Phys. **59** (1991), 619.
20) C. Clanet and J. C Lasheras, J. Fluid Mech. **383** (1999), 307.
21) J. C Sartorelli, W. M. Gonçalves and R. D. Pinto, Phys. Rev. **E49** (1994), 49.